Hindawi Publishing Corporation
Journal of Nanomaterials
Volume 2016, Article ID 5140219, 13 pages
http://dx.doi.org/10.1155/2016/5140219

Research Article

Preparation of Lanthanum Oxide and Lanthanum Oxycarbonate Layers on Titanium by Electrodeposition with Organic Solution

Jeonghee Choi and Yong Hee Chung

Department of Chemistry, Hallym University, 1 Hallymdaehak-gil, Chuncheon 24252, Republic of Korea

Correspondence should be addressed to Yong Hee Chung; yhchung@hallym.ac.kr

Received 25 March 2016; Accepted 4 July 2016

Academic Editor: Lihong Jing

Layers of lanthanum oxide and lanthanum oxycarbonate were prepared on titanium by electrodeposition with organic solution. Four voltages ranging from 200 to 1000 V were applied for the electrodeposition at three concentrations of lanthanum ions. The organic solution was isobutanol and titanium foils were used as anodes and cathodes. Currents were monitored during the electrodeposition. Deposition layers were calcined at 700 K for 30 min or at 900 K for 60 and 200 min. The morphology and composition of the deposition layers were examined by scanning electron microscopy (SEM), X-ray diffraction (XRD), and X-ray photoelectron spectroscopy (XPS). Calcined deposition layers were assayed to be lanthanum oxycarbonate and lanthanum oxide. The average crystallite size was in the vicinity of 8 nm. Sizes of lanthanum oxycarbonate agglomerates in layers with 30 min electrodeposition and calcination at 700 K were ranging from 25 to 75 nm. Yields of lanthanum oxycarbonate at three concentrations of lanthanum ions were shown to be better at 400 V.

1. Introduction

Targets of actinides with a thickness of 0.24–0.57 mg/cm^2 were used in nuclear reactions induced by heavy ions [1], while those of lanthanum oxide of 1.2 g/cm^2 [2], zirconium of 12 mg/cm^2, and hafnium of 31 mg/cm^2 were used in proton-induced reactions [3]. Targets of lanthanum oxide and lanthanum oxycarbonate with a thickness of 0.24–3.0 mg/cm^2 can be used to explore cross sections of proton-induced reactions with lanthanum to produce ^{139}Ce in the energy range of 20–35 MeV, which have not been reported in previous studies [4–6].

Lanthanum oxide thin films have been prepared by chemical vaporization, spray pyrolysis, atomic layer epitaxy, and dual plasma deposition [7–10]. Lanthanum oxide and lanthanum oxycarbonate can be prepared by a thermal decomposition [11–16]. Lanthanum oxide films were reported to reveal hemocompatibility properties suitable for biomedical materials [10]. Photocatalytic activity of lanthanum oxycarbonate studied in a degradation of methyl orange aqueous solution under ultraviolet light irradiation can be applied to wastewater purification [11]. Lanthanum oxycarbonate can be used for sensing chemoresistive CO_2 gas [16]. Thin layers of actinides can be prepared by molecular plating that is the electrodeposition performed in organic solutions [1, 17, 18]. The electrodeposition of actinides in aqueous or organic solutions has been known to present a complicated mechanism [19, 20]. This is due to the fact that the actinide elements are too electropositive to be reduced as metals at the cathode. The electrodeposition from aqueous solutions of actinides happens by a precipitation process in a layer of hydroxyl ions formed at the cathode surface and results in the oxyhydroxide compounds. Since the lanthanum element is very electropositive just like the actinide elements, its hydrolytic compound could be produced by molecular plating and be changed to lanthanum oxide by calcination.

In the present work lanthanum oxide and lanthanum oxycarbonate layers of various thicknesses were prepared on titanium foils using electrodeposition in organic solutions of three concentrations at high voltages. Effects of electrodeposition concentration, time, and voltage on morphology of calcined layers were investigated. Titanium was chosen as

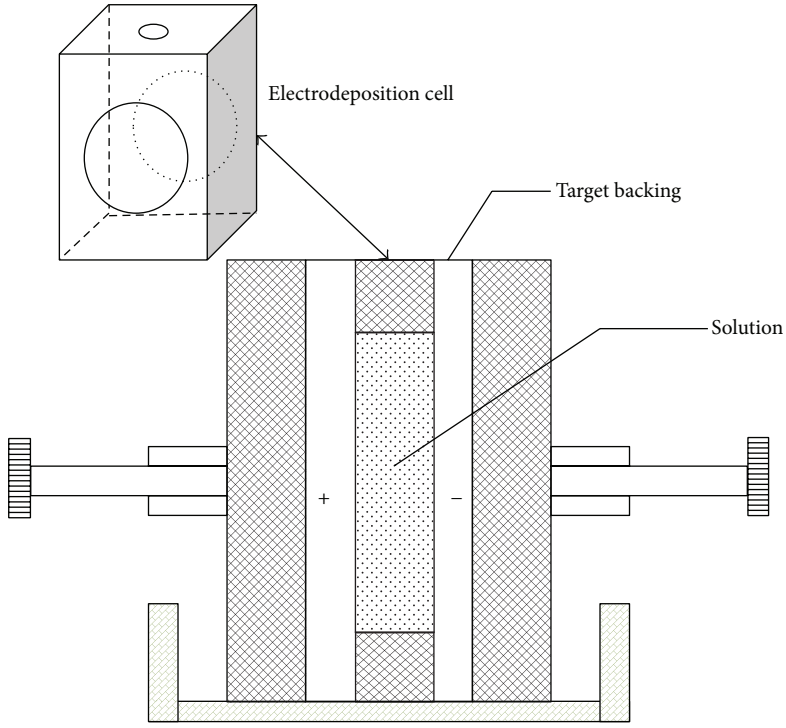

Figure 1: Schematic of an electrodeposition cell.

electrode due to the fact that it could be used to precisely determine the proton energy in proton-induced reactions [21, 22].

2. Experimental

Lanthanum nitrate hexahydrate (99.999%, Alfa Aesar) powder was dissolved in a minimal amount of distilled water and further in isobutanol. The aqueous-organic mixture was evaporated by heating above 94°C to its nearly dried state, whose composition was examined by X-ray photoelectron spectroscopy (XPS, Thermo Scientific K-Alpha$^+$ spectrometer) with an Al Kα microfocused monochromator. The dried lanthanum nitrate precursor was dissolved in isobutanol and the resulting solutions with concentrations of lanthanum ions of 0.046, 0.092, and 2.0 mg/mL, corresponding to 0.33, 0.66, and 14.5 mM, respectively, were used in the electrodeposition. The highest concentration was chosen in order to speed up electrodeposition for thicker targets with rather uniform surfaces and study how morphology of deposition layers changes with the higher concentration.

The electrodeposition was carried out at room temperature in a cell as shown in Figure 1. The cell was made of Teflon as in the other study [1]. Polished titanium foils were used as anodes and cathodes whose typical thickness was 11.4 μm. The titanium electrodes were washed consecutively by nitric acid, distilled water, and ethanol before being assembled into the cell. The electrodeposition area was 3.14 cm^2 and the distance between the electrodes was 10 mm. The cell was filled up to 3.5 mL with the organic lanthanum nitrate solution. Voltages of the electrodeposition performed at room temperature were 200, 400, 600, and 1000 V. The electrodeposition times were 30 min for 0.046 mg/mL, 30 min and 1 hr for 0.092 mg/mL, and 30 min and 8 hr for 2.0 mg/mL. The currents were monitored during the deposition time. Layers of deposited lanthanum compounds were washed consecutively by distilled water and ethanol. After being washed they were kept in ethanol for 24 hr in order to remove the residual nitrate electrolyte and dried in a drying oven at 50°C. The electrodeposited layers were calcined at 700 K for 30 min or at 900 K for 60 or 200 min. Figure 2 shows the steps involved for syntheses of lanthanum oxide and lanthanum oxycarbonate. Deposition layers with thicknesses thicker than 2.0 mg/cm^2 were prepared typically by 5 or more depositions where a calcination process was performed at 700 K for 30 min right after each deposition.

Morphology and surface compositions of electrodeposition layers were examined by scanning electron microscopy (SEM, Hitachi S-4300) and X-ray photoelectron spectroscopy (XPS, Thermo Scientific K-Alpha). Their corresponding compositions and sizes were determined from measurements by X-ray diffraction (XRD, PANalytical X'pert PRO MPD) with wavelength of Cu K_α, 1.5405 Å.

3. Results and Discussion

XPS spectrum of the lanthanum nitrate precursor with isobutanol dried on a Ti foil is shown in Figure 3(a). XPS spectra of electrodeposition layers are shown in Figures 3(b)–3(d) which were obtained without calcination, with 30 min calcination at 700 K, and with 1 hr calcination at 900 K, respectively. Figure 3(a) shows photoelectron peaks of bulk

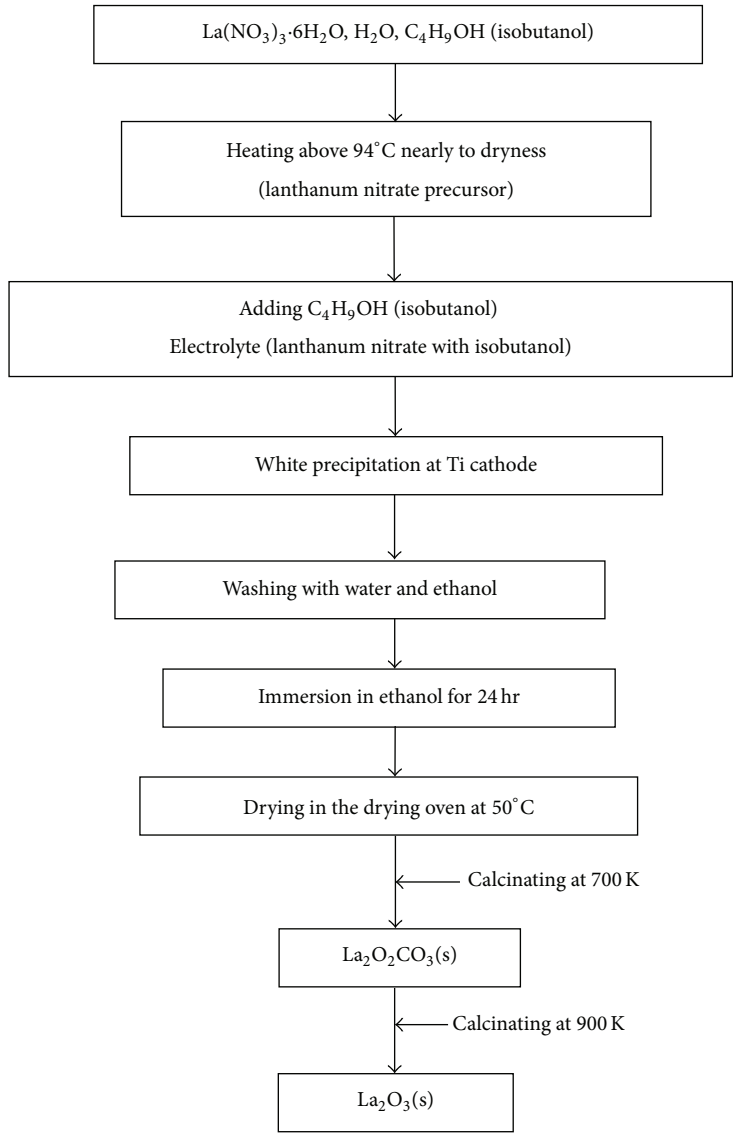

Figure 2: Chart for syntheses of lanthanum oxide and lanthanum oxycarbonate.

Table 1: Elemental composition (atomic%) obtained from XPS spectra for lanthanum nitrate precursor and electrodeposition layers.

Major element* (atomic%)	Lanthanum nitrate precursor	Layers			
		Without calcination	700 K 30 m	900 K 1 hr	900 K 200 m
La	4.5	11.6	15.0	14.4	18.2
O	61.0	55.2	56.1	59.6	61.9
C	32.8	33.2	28.9	25.9	19.9
N	1.6				

*Titanium excluded in elemental compositions.

La 3d and 4p, N 1s, O 1s, C 1s, and Ti 2p. The N 1s, O 1s, and C 1s peaks are mainly due to nitrate and isobutanol. The Ti 2p peak originates from the Ti foil. Any significant impurities were not found in the organic electrolyte. Figures 3(b)–3(d) show photoelectron peaks of La 3d and 4p, O 1s, and C 1s and their corresponding elemental compositions are listed in Table 1. As shown in Figures 3(b)–3(d) and Table 1, the carbon contents in the layers decrease as calcination temperature and time increase. Their corresponding La $3d_{5/2}$ and $3d_{3/2}$ peaks are shown in Figures 4(a) and 4(b).

The La $3d_{5/2}$ peaks for the lanthanum nitrate precursor and three layers in Figure 4(a) are at 839.6, 835.6, 834.5,

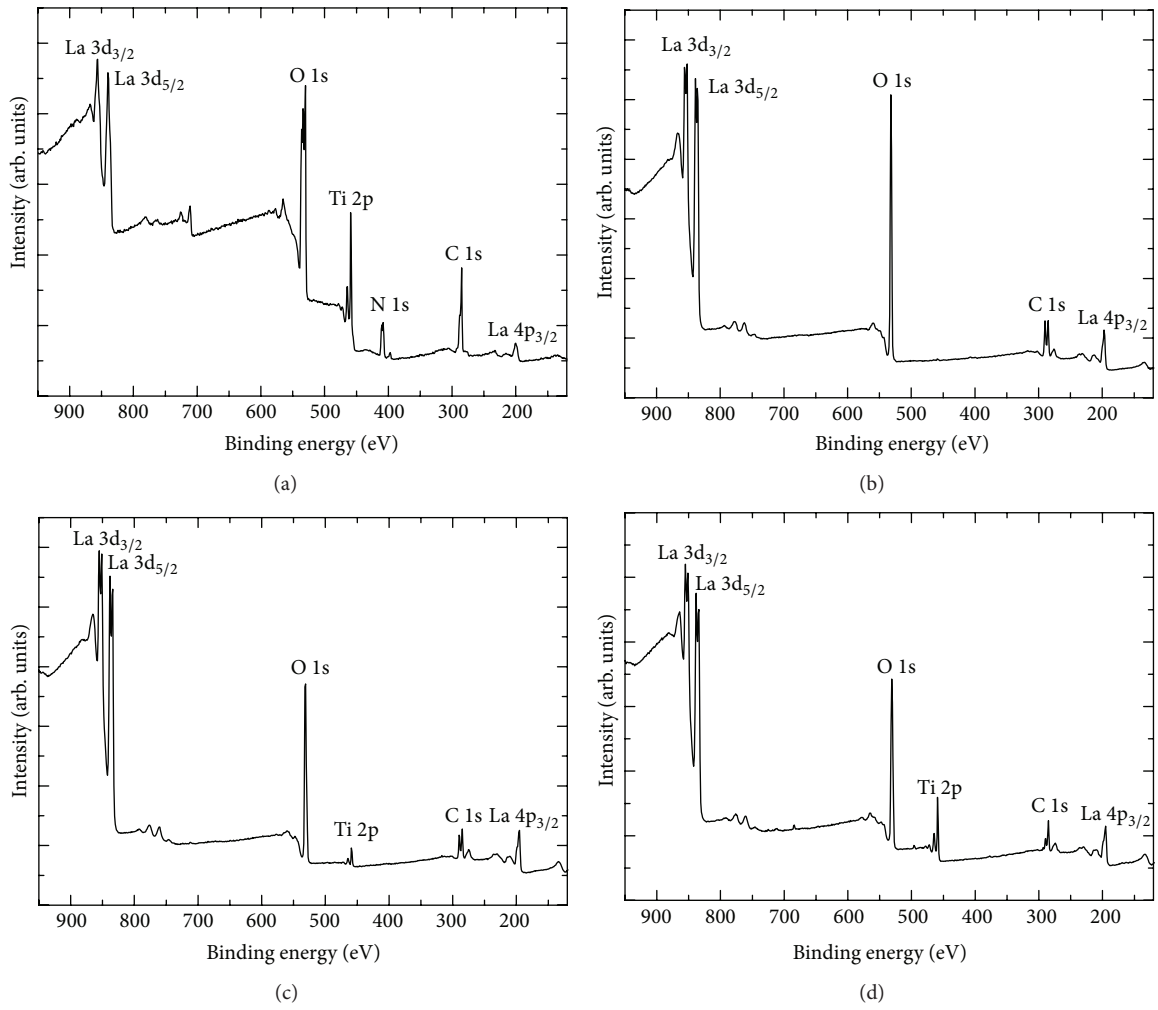

Figure 3: XPS spectra of (a) lanthanum nitrate precursor dried on Ti and layers on Ti electrodeposited at 1000 V (b) without calcination, (c) calcined at 700 K for 30 min, and (d) calcined at 900 K for 1 hr.

and 834.4 eV, respectively, while their corresponding $3d_{3/2}$ peaks in Figure 4(b) are at 856.5, 852.5, 851.4, and 851.2 eV, respectively. The La 3d peaks for the calcined layers in Figures 4(a) and 4(b) match well within 0.2 eV, implying that they have a similar chemical composition. The La 3d peaks for the layer without calcination are located at higher binding energies by 1.1–1.3 eV, which indicates that its composition is different from those of the calcined layers. The separation between La $3d_{5/2}$ and $3d_{3/2}$ peaks in the layers with or without calcination is 16.8–16.9 eV and the corresponding separation in the lanthanum nitrate precursor is 16.9 eV. Both of their satellite peaks for the calcined layers are located at higher binding energies by 3.8–3.9 eV, while those for the layer without calcination appear at higher binding energies by 3.3–3.4 eV. The broad La 3d peaks of the lanthanum nitrate precursor in Figures 4(a) and 4(b) reveal its bulk properties.

Figure 5 shows the wide-angle X-ray diffraction (XRD) patterns of three layers on Ti foils electrodeposited for 30 min at 400 V (a) without calcination, (b) calcined at 700 K for 30 min, and (c) calcined at 900 K for 200 min. The layer without calcination in Figure 5(a) shows hexagonal Ti with crystal faces of (100), (002), (101), and (102) due to the Ti foil. Measured relative intensities of diffraction peaks in Figure 5(b) at $2\theta = 13.0^\circ$, 22.8°, 26.3°, 29.5°, 31.2°, 40.1°, 41.3°, 44.4°, 52.4°, and 54.6° were 75.1, 39.3, 17.1, 100, 26.8, 36.7, 13.5, 17.9, 8.2, and 10.7%, respectively. All of them can be indexed mainly to the monoclinic structure of $La_2O_2CO_3$ with lattice constants $a = 4.0803$ Å, $b = 13.5090$ Å, and $c = 4.0720$ Å (reference code 00-048-1113) and partially to the tetragonal structure of $La_2O_2CO_3$ with lattice constants $a = 4.0630$ Å, $b = 4.0630$ Å, and $c = 13.5000$ Å (reference code 00-023-0320), implying that the layer calcined at 700 K for 30 min is $La_2O_2CO_3$ with mixed monoclinic and tetragonal phases. The average particle size was estimated using Scherrer equation [11, 23]:

$$D = \frac{K\lambda}{\beta \cos\theta}, \tag{1}$$

where D is the average particle size, K is the dimensionless shape factor whose typical value is about 0.9, λ is the X-ray wavelength used in XRD (Cu $K_\alpha = 1.5405$ Å), β is the broadening of the observed diffraction line at half the

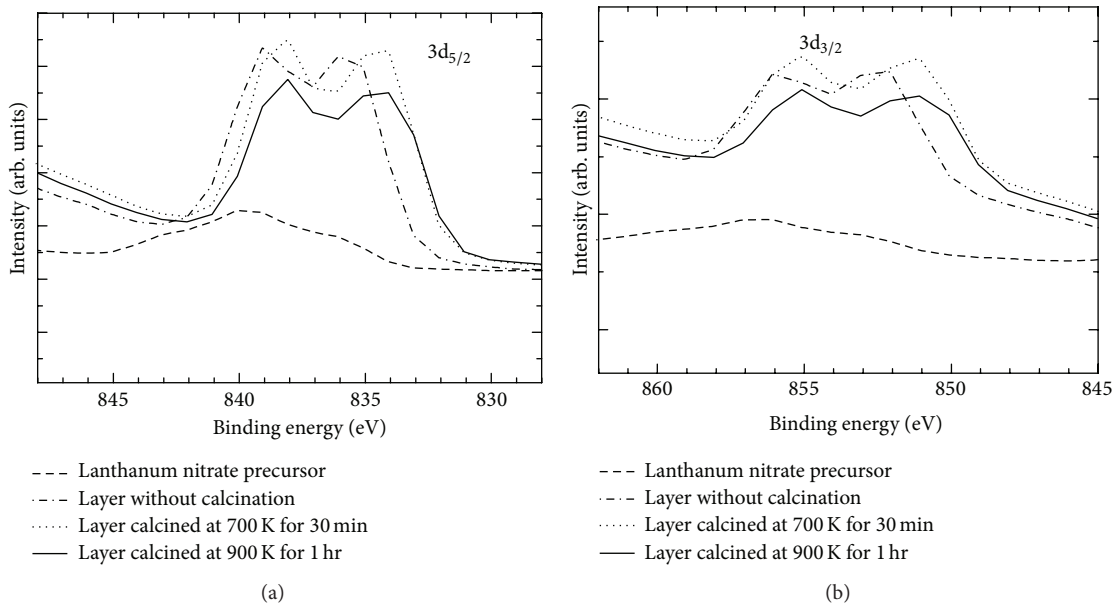

FIGURE 4: XPS spectra of (a) La $3d_{5/2}$ and (b) La $3d_{3/2}$ peaks in Figures 3(a)–3(d): dashed lines (Figure 3(a)); dash-and-dot lines (Figure 3(b)); dotted lines (Figure 3(c)); and solid lines (Figure 3(d)).

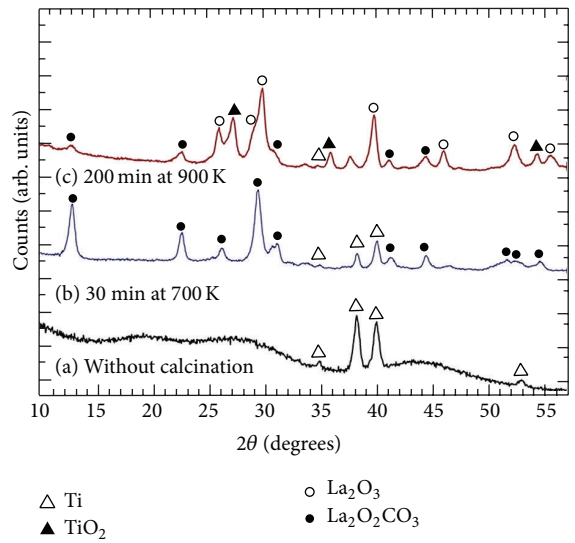

FIGURE 5: X-ray diffraction patterns of three layers on Ti electrodeposited at 400 V: (a) without calcination and with calcination (b) at 700 K for 30 min and (c) at 900 K for 200 min.

maximum intensity in radians, and θ is the Bragg angle. Using the peaks at 2θ = 13.0°, 22.8°, 26.3°, 29.5°, 31.2°, 40.1°, 41.3°, 44.4°, 52.4°, and 54.6°, the average crystallite size of the layer calcined at 700 K for 30 min was deduced to be 16 ± 3 nm.

The XRD pattern of the layer calcined at 900 K for 200 min shown in Figure 5(c) confirms partial decomposition of $La_2O_2CO_3$ to La_2O_3. The decomposition reaction can be written as $La_2O_2CO_3(s) \rightarrow La_2O_3(s) + CO_2(g)$, which was reported to occur above 993 K [12]. Diffraction peaks in Figure 5(c) at 2θ = 27.6°, 36.2°, 41.4°, and 54.6° can be indexed to the tetragonal structure of TiO_2 produced from calcination of Ti foil at 900 K. Dominant diffraction peaks at 2θ = 26.1°, 29.3°, 29.9°, 39.8°, 46.0°, 52.2°, 55.5°, and 55.9° can be indexed to the hexagonal structure of La_2O_3 with lattice constants a = 3.9373 Å, b = 3.9373 Å, and c = 6.1299 Å (reference code 01-074-2430), while significant peaks at 2θ = 12.9°, 22.7°, 31.0°, 39.9°, and 44.4° can be indexed to the monoclinic structure of $La_2O_2CO_3$. The scaling factors of La_2O_3 and $La_2O_2CO_3$ were estimated to be 1.024 and 0.399, respectively, implying that the layer calcined at 900 K for 200 min consists of 72% La_2O_3 and 28% $La_2O_2CO_3$. Using the peaks at 2θ = 26.1°, 29.3°, 29.9°, 46.0°, 52.2°, and 55.5° for La_2O_3, the corresponding average crystallite size was deduced to be 9 ± 3 nm. Using the peaks at 2θ = 12.9°, 22.7°, 31.0°, and 44.4° for $La_2O_2CO_3$,

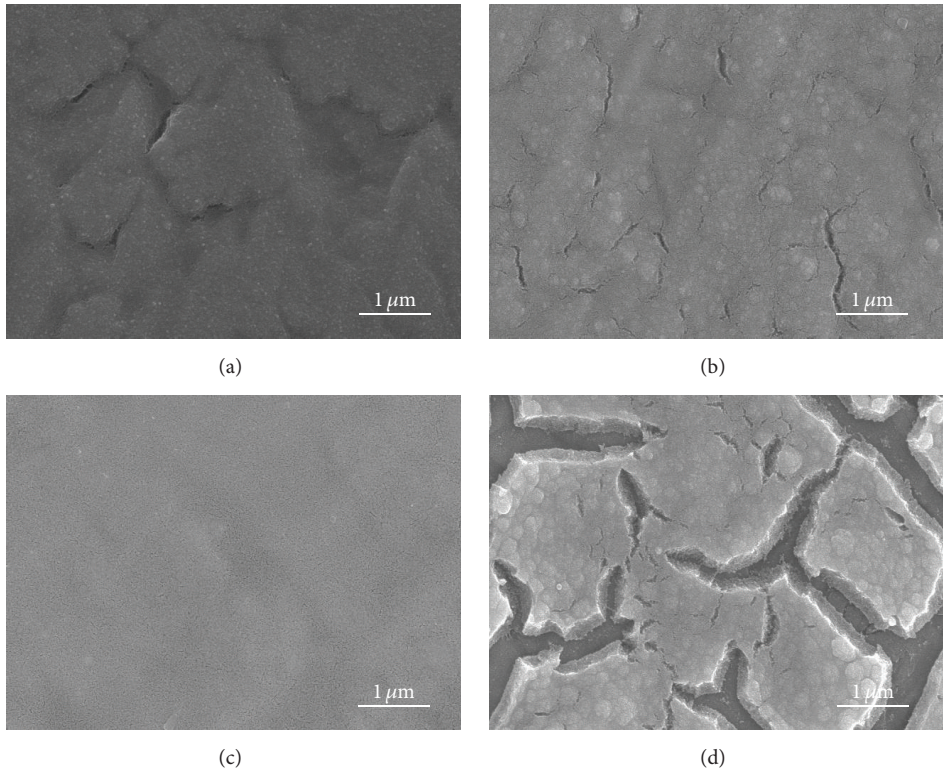

Figure 6: SEM micrographs of $La_2O_2CO_3$ layers calcined at 700 K for 30 min after 30 min electrodeposition of 0.046 mg/mL of La^{3+} ions on Ti at (a) 200 V, (b) 400 V, (c) 600 V, and (d) 1000 V.

the corresponding average crystallite size calcined at 900 K for 200 min was deduced to be 8 ± 1 nm. The average particle size of $La_2O_2CO_3$ nanoparticles decreases from 16 to 8 nm as calcination temperature and time increase from 700 to 900 K and from 30 to 200 min, respectively.

SEM micrographs of $La_2O_2CO_3$ layers on Ti foils calcined at 700 K for 30 min after 30 min electrodepositions of La^{3+} ions of 0.046, 0.092, and 2.0 mg/mL at 200, 400, 600, and 1000 V are shown in Figures 6–8, respectively. SEM micrographs of $La_2O_2CO_3$ layers of the corresponding concentrations obtained by two electrodeposition and calcination steps are shown in Figures 9–11. The layers in Figures 9–11 were obtained by performing two steps of the electrodeposition and subsequent 30 min calcination and the corresponding deposition times were 30 and 30 min, 30 min and 1 hr, and 30 min and 8 hr, respectively. Figure 6 shows lanthanum oxycarbonate layers containing agglomerates with sizes ranging between 37 and 75 nm. Lanthanum oxycarbonate layers in Figure 7 contain agglomerates with size ranging between 30 and 75 nm, while those in Figure 8 have agglomerates with size ranging between 25 and 62 nm. Figures 9–11 show the larger agglomerates whose sizes increase to 66–330, 66–1300, and 44–2200 nm, respectively. Lanthanum oxycarbonate nanoparticles with agglomerates of various sizes can be tested as sensing materials in photocatalytic activity and wastewater purification.

Currents of 30 min electrodepositions at 200, 400, 600, and 1000 V with 0.046, 0.092, and 2.0 mg/mL of La^{3+} ions are shown in Figures 12–14, respectively. Figure 12 shows that currents start to increase during the process but at 600 V start to fall after about 6 min. The corresponding accumulated current is highest at 400 V and lowest at 200 V. Figure 13 shows that currents start to increase during the process but at 400 V start to fall after about 10 min and to sharply drop after about 20 min. The corresponding accumulated current is highest at 1000 V and lowest at 200 V. Figure 14 shows that all currents start to increase during the process. The values of the corresponding accumulated currents are close to one another.

Yields of 30 min electrodepositions at 200, 400, 600, and 1000 V with 0.046, 0.092, and 2.0 mg/mL of La^{3+} ions are shown in Figures 15–17, respectively. The yields in Figure 15 are close to ~70% at higher voltages which appears to be slightly higher than ~60% at 200 V. The corresponding thicknesses were 0.04–0.05 mg/cm^2. Figures 16 and 17 show that the yields are highest at 400 V. The corresponding thicknesses in Figures 16 and 17 were 0.09–0.13 and 0.38–0.46 mg/cm^2, respectively. The yields of lanthanum oxycarbonate nanoparticles at three concentrations of lanthanum ions were shown to be better at 400 V, even though their morphology varies slightly with the voltage. Using 5 or 6 steps of the 30 min electrodeposition and subsequent 30 min calcination process, thicker layers of $La_2O_2CO_3$ were prepared at 200, 400, 600, and 1000 V and the corresponding thicknesses were 2.0, 2.3, 2.3, and 2.0 mg/cm^2, respectively. The results are shown in Figure 18. The layer obtained at 400 V is covered with

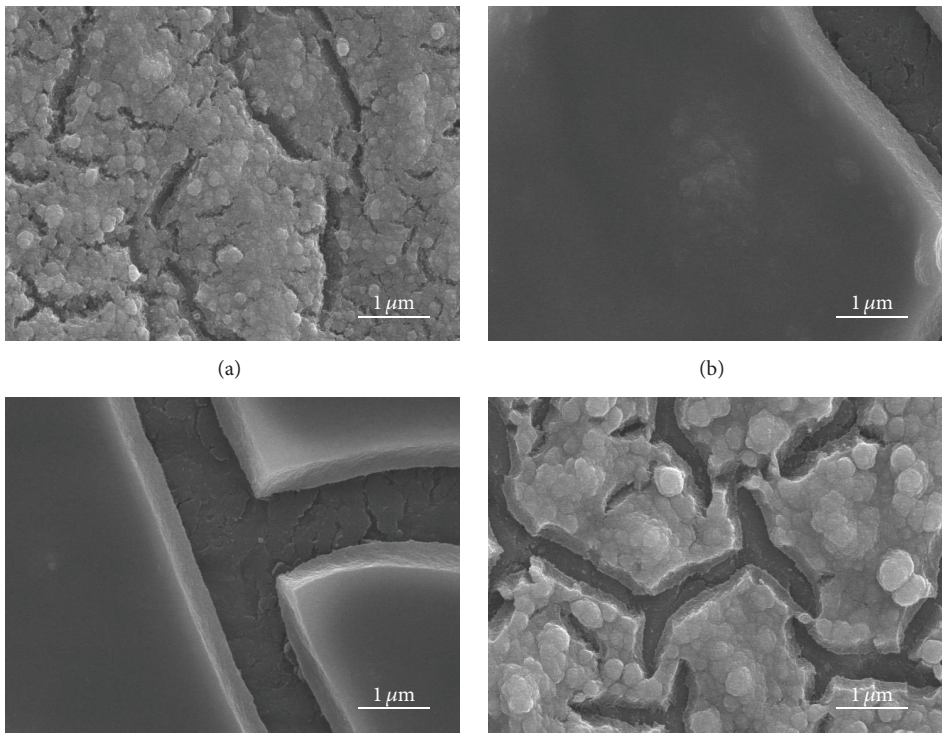

FIGURE 7: SEM micrographs of $La_2O_2CO_3$ layers calcined at 700 K for 30 min after 30 min electrodeposition of 0.092 mg/mL of La^{3+} ions on Ti at (a) 200 V, (b) 400 V, (c) 600 V, and (d) 1000 V.

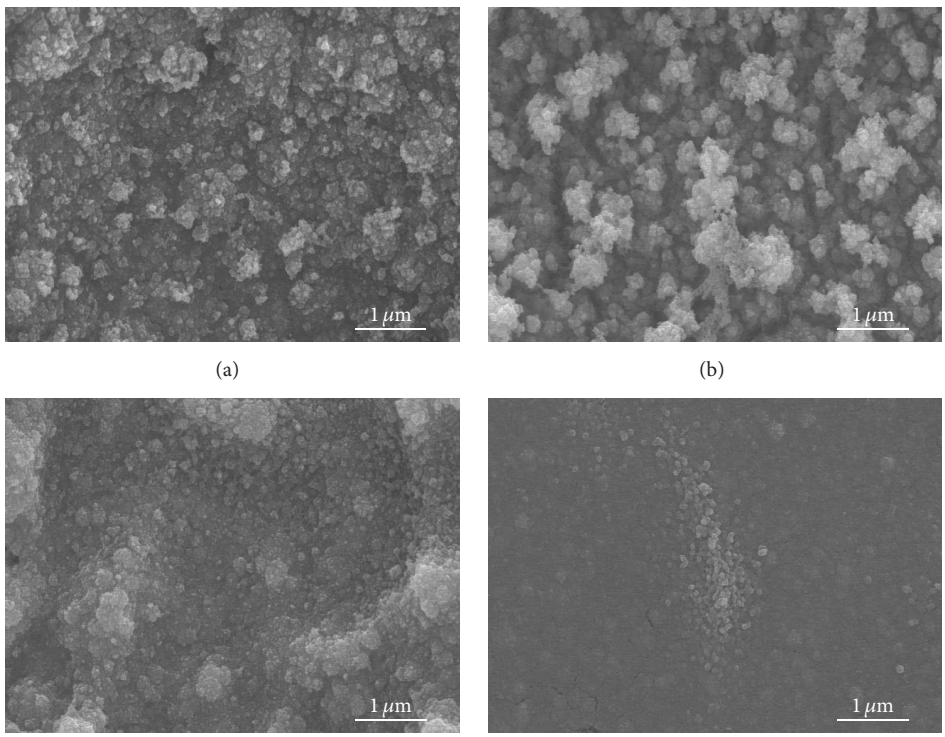

FIGURE 8: SEM micrographs of $La_2O_2CO_3$ layers calcined at 700 K for 30 min after 30 min electrodeposition of 2.0 mg/mL of La^{3+} ions on Ti at (a) 200 V, (b) 400 V, (c) 600 V, and (d) 1000 V.

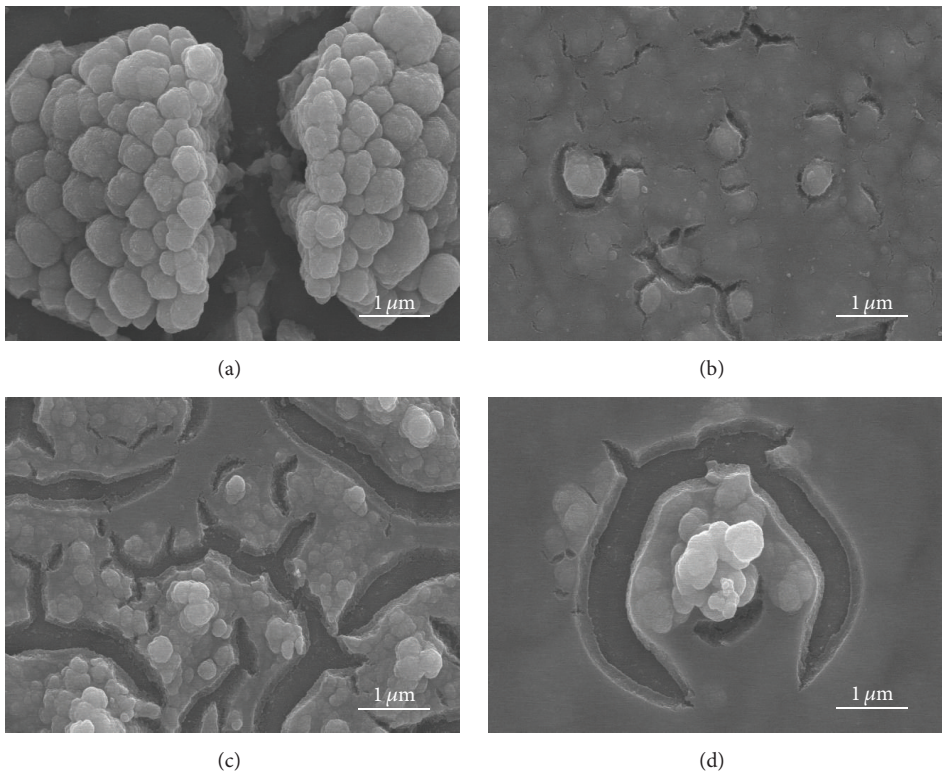

FIGURE 9: SEM micrographs of $La_2O_2CO_3$ layers calcined at 700 K for 30 min after two 30 min electrodepositions of 0.046 mg/mL of La^{3+} ions on Ti at (a) 200 V, (b) 400 V, (c) 600 V, and (d) 1000 V.

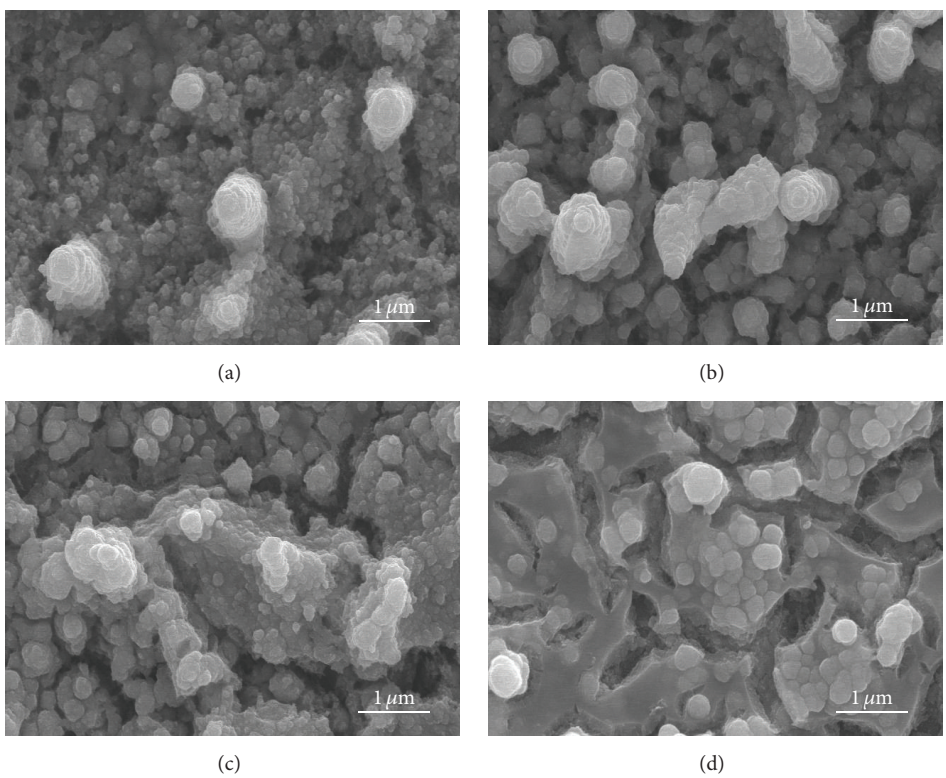

FIGURE 10: SEM micrographs of $La_2O_2CO_3$ layers calcined at 700 K for 30 min after 30 min and 1 hr electrodeposition of 0.092 mg/mL of La^{3+} ions on Ti at (a) 200 V, (b) 400 V, (c) 600 V, and (d) 1000 V.

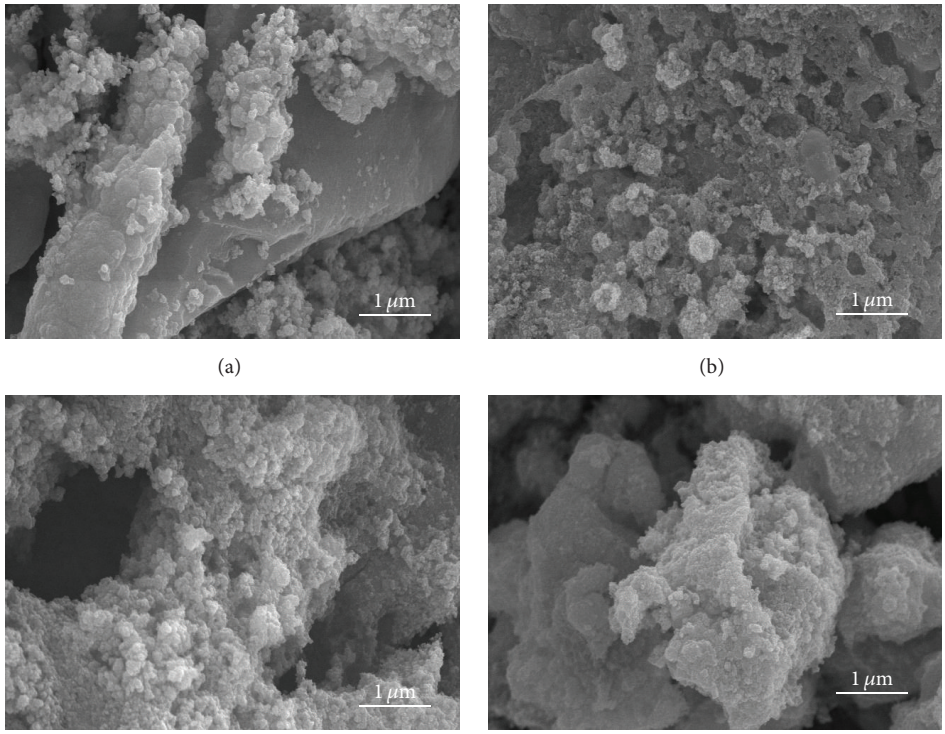

FIGURE 11: SEM micrographs of $La_2O_2CO_3$ layers calcined at 700 K for 30 min after 30 min and 8 hr electrodeposition of 2.0 mg/mL of La^{3+} ions on Ti at (a) 200 V, (b) 400 V, (c) 600 V, and (d) 1000 V.

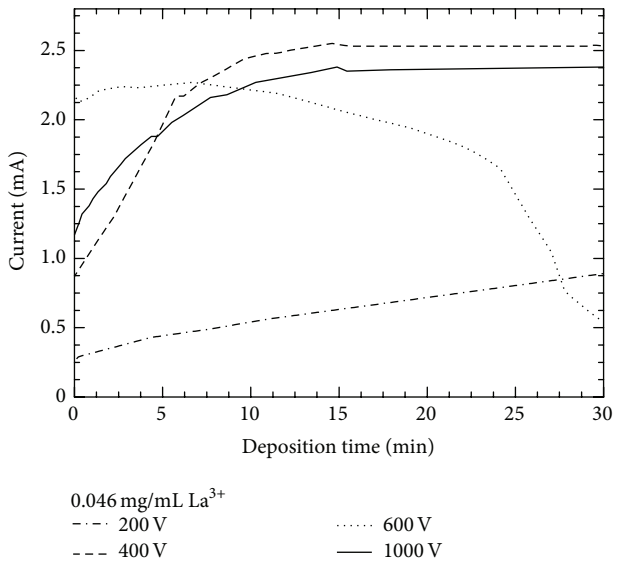

FIGURE 12: Currents of 30 min depositions with 0.046 mg/mL of La^{3+} ions at 200, 400, 600, and 1000 V.

finer agglomerates while the others contain a little larger agglomerates.

4. Conclusions

Layers of $La_2O_2CO_3$ with various thicknesses ranging from 0.04 to 2.3 mg/cm^2 along with La_2O_3 layers have been produced on Ti by electrodeposition of La^{3+} ions in isobutanol and subsequent calcination. Layers calcined at 700 K for 30 min turned out to be $La_2O_2CO_3$ mainly with monoclinic phase and partially with tetragonal phase. Layers calcined at 900 K for 200 min were observed to contain 72% La_2O_3 with hexagonal phase and 28% $La_2O_2CO_3$. The average particle size of $La_2O_2CO_3$ decreases from 16 to 8 nm as calcination

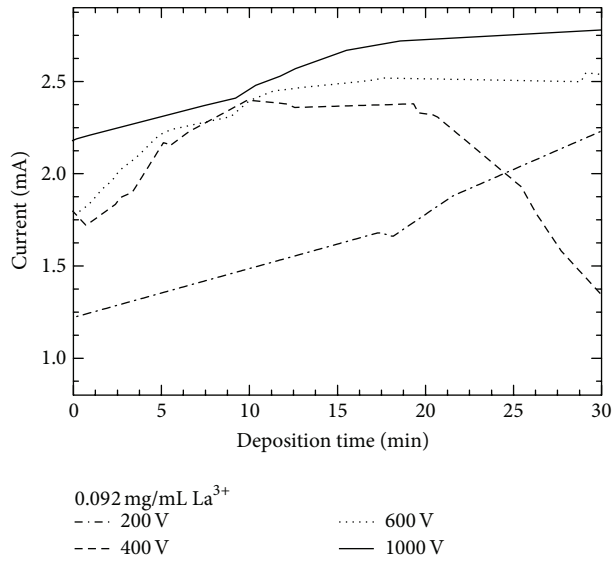

Figure 13: Currents of 30 min depositions with 0.092 mg/mL of La^{3+} ions at 200, 400, 600, and 1000 V.

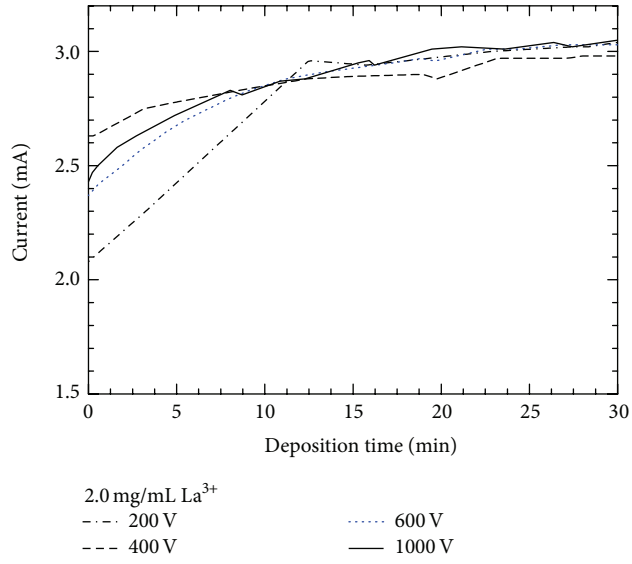

Figure 14: Currents of 30 min depositions with 2.0 mg/mL of La^{3+} ions at 200, 400, 600, and 1000 V.

temperature and time increases from 700 to 900 K and from 30 to 200 min, respectively. Dependence of the layer thickness on the electrodeposition voltage in this range was not pronounced, even though the morphology varies slightly with the voltage. Currents and yields with three concentrations of lanthanum ions were shown to be enhanced at 400 V. The layer thicknesses with lanthanum concentrations of 0.046, 0.092, and 2.0 mg/mL were 0.04–0.05, 0.09–0.13, and 0.38–0.46 mg/cm^2, respectively. The sizes of their agglomerates were ranging from 25 to 75 nm. Using 5 or 6 steps of the 30 min electrodeposition and subsequent 30 min calcination process, thicker layers of $La_2O_2CO_3$ were prepared at 200, 400, 600, and 1000 V and the corresponding thicknesses were 2.0, 2.3, 2.3, and 2.0 mg/cm^2, respectively. The sizes of their agglomerates were ranging from 44 to 2200 nm. Lanthanum oxycarbonate nanoparticles with agglomerates of various sizes are to be tested as sensing materials in photocatalytic activity and wastewater purification.

Competing Interests

The authors declare that they have no competing interests.

Acknowledgments

This work was financially supported by Hallym University (HRF-201501-011).

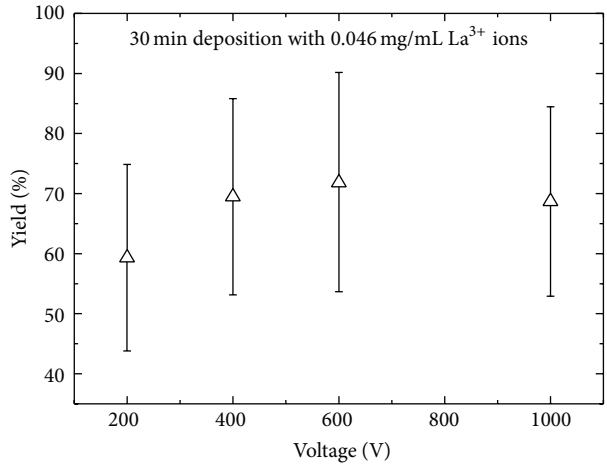

Figure 15: Yields of 30 min depositions with 0.046 mg/mL of La^{3+} ions at 200, 400, 600, and 1000 V.

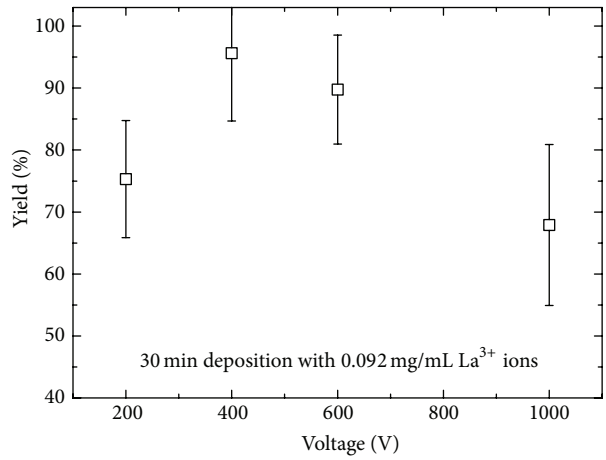

Figure 16: Yields of 30 min depositions with 0.092 mg/mL of La^{3+} ions at 200, 400, 600, and 1000 V.

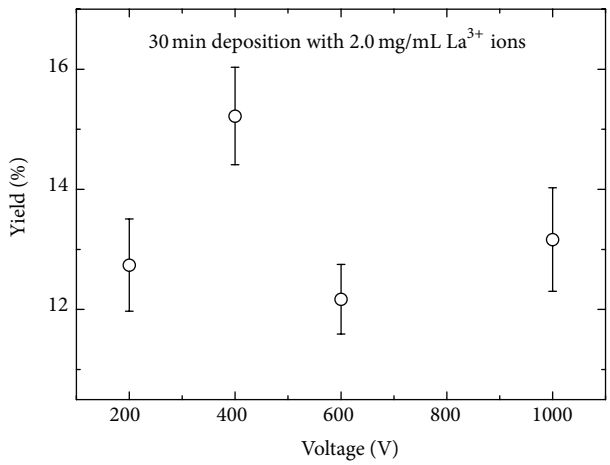

Figure 17: Yields of 30 min depositions with 2.0 mg/mL of La^{3+} ions at 200, 400, 600, and 1000 V.

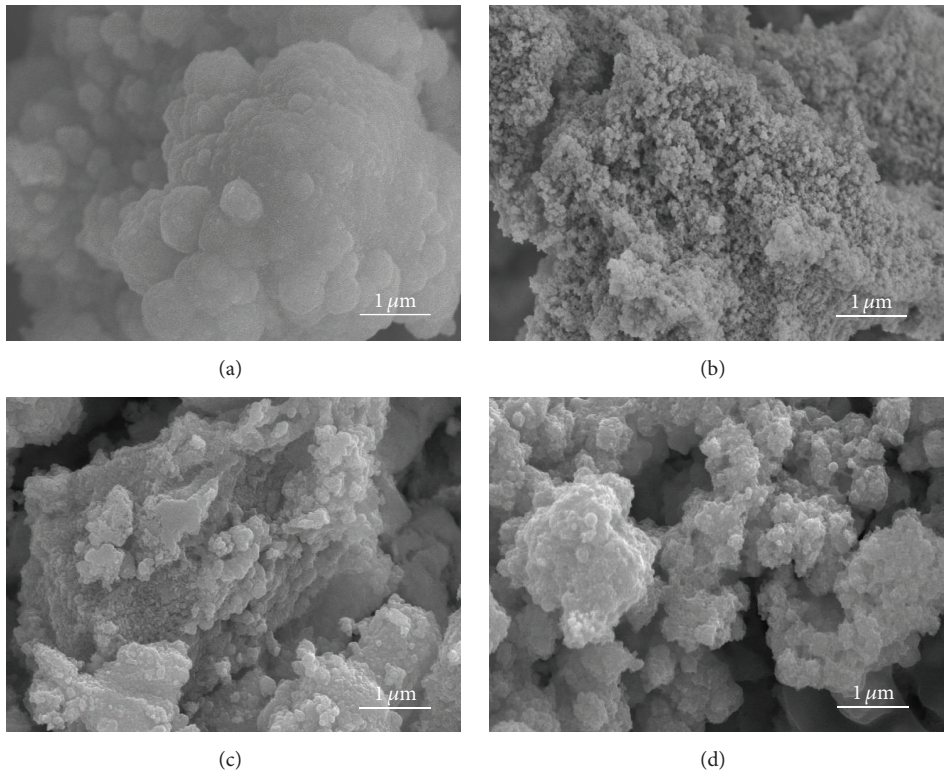

Figure 18: SEM micrographs of $La_2O_2CO_3$ layers obtained by 5-6 steps of 30 min calcination at 700 K following 30 min electrodeposition of 2.0 mg/mL of La^{3+} ions on Ti at (a) 200 V, (b) 400 V, (c) 600 V, and (d) 1000 V.

References

[1] Y. V. Lobanov, G. V. Buklanov, F. S. Abdullin et al., "Targets of uranium, plutonium, and curium for heavy-element research," *Nuclear Instruments and Methods in Physics Research, Section A: Accelerators, Spectrometers, Detectors and Associated Equipment*, vol. 397, no. 1, pp. 26–29, 1997.

[2] C. Vermeulen, G. F. Steyn, F. M. Nortier, F. Szelecsényi, Z. Kovács, and S. M. Qaim, "Production of ^{139}Ce by proton-induced reactions on ^{141}Pr and ^{nat}La," *Nuclear Instruments and Methods in Physics Research Section B: Beam Interactions with Materials and Atoms*, vol. 255, no. 2, pp. 331–337, 2007.

[3] M. Murakami, H. Haba, S. Goto, J. Kanaya, and H. Kudo, "Production cross sections of niobium and tantalum isotopes in proton-induced reactions on ^{nat}Zr and ^{nat}Hf up to 14 MeV," *Applied Radiation and Isotopes*, vol. 90, pp. 149–157, 2014.

[4] J. Wing and J. R. Huizenga, "(*p, n*) cross sections of V^{51}, Cr^{52}, Cu^{63}, Cu^{65}, Ag^{107}, Ag^{109}, Cd^{111}, Cd^{114}, and La^{139} from 5 to 10.5 MeV," *Physical Review*, vol. 128, no. 1, pp. 280–290, 1962.

[5] H. E. Hassan, F. S. Al-Saleh, K. F. Hassan, A. Sayaed, and Z. A. Saleh, "Proton induced reactions on Tb-159 and La-139 for producing Dy and Ce-139," in *Proceedings of the 6th International Conference on Nuclear and Particle Physics*, p. 209, Luxor, Egypt, 2007.

[6] G. Albouy, M. Gusakow, N. Poffé, H. Sergolle, and L. Valentin, "Réactions (p, n) à moyenne énergie," *Journal de Physique et le Radium*, vol. 23, no. 12, pp. 1000–1002, 1962.

[7] H. C. Aspinall, J. Gaskell, P. A. Williams et al., "Growth of lanthanum oxide thin films by liquid injection MOCVD using a novel lanthanum alkoxide precursor," *Chemical Vapor Deposition*, vol. 10, no. 1, pp. 13–17, 2004.

[8] M. Nieminen, M. Putkonen, and L. Niinistö, "Formation and stability of lanthanum oxide thin films deposited from β-diketonate precursor," *Applied Surface Science*, vol. 174, no. 2, pp. 155–165, 2001.

[9] S. S. Kale, K. R. Jadhav, P. S. Patil, T. P. Gujar, and C. D. Lokhande, "Characterizations of spray-deposited lanthanum oxide (La_2O_3) thin films," *Materials Letters*, vol. 59, no. 24-25, pp. 3007–3009, 2005.

[10] F. J. Jing, L. Wang, Y. W. Liu et al., "Hemocompatibility of lanthanum oxide films fabricated by dual plasma deposition," *Thin Solid Films*, vol. 515, no. 3, pp. 1219–1222, 2006.

[11] M. Ghiasi and A. Malekzadeh, "Synthesis, characterization and photocatalytic properties of lanthanum oxy-carbonate, lanthanum oxide and lanthanum hydroxide nanoparticles," *Superlattices and Microstructures*, vol. 77, pp. 295–304, 2015.

[12] A. N. Shirsat, M. Ali, K. N. G. Kaimal, S. R. Bharadwaj, and D. Das, "Thermochemistry of $La_2O_2CO_3$ decomposition," *Thermochimica Acta*, vol. 399, no. 1-2, pp. 167–170, 2003.

[13] Q. Shi, Z. Peng, W. Chen, and N. Zhang, "$La_2O_2CO_3$ supported Ni-Fe catalysts for hydrogen production from steam reforming of ethanol," *Journal of Rare Earths*, vol. 29, no. 9, pp. 861–865, 2011.

[14] H. Niu, Q. Min, Z. Tao et al., "One-pot facile synthesis and optical properties of porous $La_2O_2CO_3$ hollow microspheres," *Journal of Alloys and Compounds*, vol. 509, no. 3, pp. 744–747, 2011.

[15] A. Pons, J. Jouin, E. Béchade et al., "Study of the formation of the apatite-type phases $La_{9.33+x}(SiO_4)6O_{2+3x/2}$ synthesized from

a lanthanum oxycarbonate $La_2O_2CO_3$," *Solid State Sciences*, vol. 38, pp. 150–155, 2014.

[16] G. Chen, B. Han, S. Deng, Y. Wang, and Y. Wang, "Lanthanum dioxide carbonate $La_2O_2CO_3$ nanorods as a sensing material for chemoresistive CO_2 gas sensor," *Electrochimica Acta*, vol. 127, pp. 355–361, 2014.

[17] W. Parker and M. Colonomos, "Preparation of thin layers of ^{237}Np for absolute counting and fission detectors," *Nuclear Instruments and Methods*, vol. 66, no. 1, pp. 137–140, 1968.

[18] K. B. Lee, J. M. Lee, T. S. Park, and P.-J. Oh, "Preparation and activity measurement of electrodeposited alpha-emitting sources," *Applied Radiation and Isotopes*, vol. 64, no. 10-11, pp. 1260–1264, 2006.

[19] P. G. Hansen, "The conditions for electrodeposition of insoluble hydroxides at a cathode surface: a theoretical investigation," *Journal of Inorganic and Nuclear Chemistry*, vol. 12, no. 1-2, pp. 30–37, 1959.

[20] M. T. Crespo, "A review of electrodeposition methods for the preparation of alpha-radiation sources," *Applied Radiation and Isotopes*, vol. 70, no. 1, pp. 210–215, 2012.

[21] S. Takács, F. Tárkányi, M. Sonck, and A. Hermanne, "New cross-sections and intercomparison of proton monitor reactions on Ti, Ni and Cu," *Nuclear Instruments and Methods in Physics Research, Section B: Beam Interactions with Materials and Atoms*, vol. 188, no. 1–4, pp. 106–111, 2002.

[22] K. Gul, A. Hermanne, M. G. Mustafa et al., "Charged particle cross-section database for medical radioisotope production: diagnostic and monitor reactions," Tech. Rep. IAEA-TECDOC-1211, International Atomic Energy Agency, Vienna, Austria, 2001.

[23] M. Salavati-Niasari, G. Hosseinzadeh, and F. Davar, "Synthesis of lanthanum hydroxide and lanthanum oxide nanoparticles by sonochemical method," *Journal of Alloys and Compounds*, vol. 509, no. 10, pp. 4098–4103, 2011.